Published in final edited form as:
Cell Rep. 2012 January 26; 1(1): 2–12. doi:10.1016/j.celrep.2011.11.001.

Mutations in the novel protein PRRT2 cause paroxysmal kinesigenic dyskinesia with infantile convulsions

Hsien-Yang Lee[1], **Yong Huang**[1,2], **Nadine Bruneau**[3], **Patrice Roll**[4], **Elisha D.O. Roberson**[5], **Mark Hermann**[1], **Emily Quinn**[1,2], **James Maas**[1], **Robert Edwards**[1], **Tetsuo Ashizawa**[6], **Betul Baykan**[7], **Kailash Bhatia**[8], **Susan Bressman**[9], **Michiko K. Bruno**[1,10], **Ewout R. Brunt**[11], **Roberto Caraballo**[12], **Bernard Echenne**[13], **Natalio Fejerman**[12], **Steve Frucht**[14], **Christina A. Gurnett**[15], **Edouard Hirsch**[16], **Henry Houlden**[8], **Joseph Jankovic**[17], **Wei-Ling Lee**[18], **David R. Lynch**[19], **Shehla Mohamed**[20], **Ulrich Müller**[21], **Mark P. Nespeca**[22], **David Renner**[23], **Jacques Rochette**[24], **Gabrielle Rudolf**[16], **Shinji Saiki**[25,26], **Bing-Wen Soong**[27], **Kathryn J. Swoboda**[23], **Sam Tucker**[19], **Nicholas Wood**[8], **Michael Hanna**[8,28], **Anne Bowcock**[5,28], **Pierre Szepetowski**[3,28], **Ying-Hui Fu**[1,28], and **Louis J. Ptáček**[1,2,28]

[1]Department of Neurology, UCSF, San Francisco, California, 94158

[2]Howard Hughes Medical Institute, San Francisco, California, 94158

[3]Institut de Neurobiologie de la Méditerranée, INMED. Inserm U901. Université de la Méditerranée. Marseille, France

[4]INSERM UMR_S910, Université de la Méditerranée, Marseille, France

[5]Division of Human Genetics, Department of Genetics, Washington University School of Medicine, Saint Louis, MO, 63110

[6]Department of Neurology, University of Florida, Gainesville, Florida 32611

[7]Department of Neurology, Istanbul University, Millet Cad 34390 Istanbul Turkey

[8]Institute of Neurology, University College London, London, WC1N 3BG

[9]Department of Neurology, Beth Israel Medical Center, New York, New York, 10003

[10]Department of Neurology, The Queen's Medical Center, Honolulu, Hawaii, 96813

[11]Department of Neurology, University Medical Centre Groningen, University of Groningen, The Netherlands, 9713 GZ

[12]Department of Neurology, Juan P. Garrahan Pediatric Hospital, Combate de los Pozos 1881. CP 1245, Buenos Aires, Argentina

[13]Service de Neuropédiatrie, Hôpital Gui de Chauliac, Montpellier, France

*Correspondence to: ying-hui.fu@ucsf.edu or ljp@ucsf.edu.
[26]Present Address: Department of Neurology, Juntendo University School of Medicine, Tokyo 113-8421,Japan

[14]Movement Disorders Center, Mount Sinai Medical Center, New York, 10029

[15]Department of Neurology, Washington University School of Medicine, St Louis, MO 63110

[16]Service de Neurologie. Hôpitaux Universitaires de Strasbourg, France

[17]Parkinson's Disease Center and Movement Disorders Clinic, Department of Neurology, Baylor College of Medicine, Houston, Texas 77030

[18]National Neuroscience Institute, Singapore

[19]Division of Neurology, Children's Hospital of Philadelphia, Philadelphia, Pa. USA, 19104

[20]Clinical Genetics, Guy's Hospital, London, SE1 9RT

[21]Institut für Humangenetik, Justus-Liebig-Universität, Giessen, Germany, D-35392

[22]Pediatric Neurology Division, Rady Children's Hospital San Diego, UCSD Department of Neuroscience, San Diego, California, 92123

[23]Department of Neurology, University of Utah, Salt Lake City, Utah, 84132

[24]Service de Génétique-INSERM UMR 925 , Université de Picardie Jules Verne, Amiens 80036-France

[25]Department of Neurology, Kanazawa Medical University, Ishikawa, Japan, 920-0293

[27]Department of Neurology, National Yang-Ming University School of Medicine and the Neurological Institute, Taipei Veterans General Hospital, Taipei, Taiwan

[28]Senior Investigator of the International Paroxysmal Kinesigenic Dyskinesia/Infantile Convulsions Collaborative Working Group

Summary

Paroxysmal Kinesigenic Dyskinesia with Infantile Convulsions (PKD/IC) is an episodic movement disorder with autosomal dominant inheritance and high penetrance, but the causative gene is unknown. We have now identified four truncating mutations involving the *PRRT2* gene in the vast majority (24/25) of well characterized families with PKD/IC. PRRT2 truncating mutations were also detected in 28 of 78 additional families. The *PRRT2* gene encodes a proline-rich transmembrane protein of unknown function that has been reported to interact with the t-SNARE, SNAP25. PRRT2 localizes to axons but not to dendritic processes in primary neuronal culture and mutants associated with PKD/IC lead to dramatically reduced PRRT2 protein levels leading ultimately to neuronal hyperexcitability that manifests *in vivo* as PKD/IC.

Introduction

The paroxysmal dyskinesias (PD) are a heterogeneous group of episodic movement disorders that can be separated on the basis of factors that precede or precipitate attacks, the nature and durations of attacks, and etiology (Bhatia, 2011; Blakeley and Jankovic, 2002). Individuals are typically completely normal between attacks. Attacks of PD and epileptic seizures share several characteristics. The syndrome of paroxysmal kinesigenic dyskinesia with infantile convulsions (PKD/IC, formerly reported as ICCA syndrome; OMIM 602066)

typically presents in the first year of life with benign, afebrile infantile convulsions that spontaneously resolve, usually by two years of age. In young childhood, these individuals begin having PKD, i.e. frequent but brief movements precipitated by sudden movements or change in velocity of movement (e.g. sitting to standing, standing to walking, walking to running). Patients may experience dozens to hundreds of PKD attacks per day. They typically last less than five or ten seconds but occasionally may be longer. Interestingly, investigators studying families with autosomal dominant infantile convulsions had recognized that these individuals also developed paroxysmal movement disorders (Szepetowski et al., 1997). Separately, investigators studying PKD, upon taking closer family histories, recognized that their families were also segregating alleles for autosomal dominant infantile convulsions (Swoboda et al., 2000). In typical PKD/IC families, variable presentation is usual and patients present either with PKD, IC, or both. Interfamilial variable expressivity also exists. Hence families with IC but no PKD were reported and the majority were considered allelic variants of PKD/IC (Caraballo et al., 2001). Similarly, many PKD families are recognized in which there is no mention of IC, perhaps because the seizures had resolved leading to presentation with an episodic movement disorder. The nature of the infantile convulsions and the paroxysmal dyskinesias has been well described (Bruno et al., 2004; Rochette et al., 2008; Swoboda et al., 2000; Szepetowski et al., 1997). The gene for PKD/IC has been mapped to chromosome 16 by many groups and extensive efforts to identify the gene have been ongoing (Bennett et al., 2000; Callenbach et al., 2005; Caraballo et al., 2001; Du et al., 2008; Kikuchi et al., 2007; Lee et al., 1998; Roll et al.; Swoboda et al., 2000; Szepetowski et al., 1997; Tomita et al., 1999; Weber et al., 2004).

After having firmly excluded by sequencing the vast majority of the one hundred and eighty known or predicted genes in the critical chromosome 16 locus for PKD/IC, we set out to perform whole genome sequencing from one affected member each from six of our most well characterized families. Upon examining this sequence, we identified potential mutations in a gene called proline-rich transmembrane protein 2 (*PRRT2*, Entrez Gene: 112476). We chose to examine this gene in a larger collection of well characterized families from an international PKD/IC consortium. Our interest in *PRRT2* was strengthened for a number of reasons. We've shown that a mouse model of PNKD exhibits dysregulation of dopamine signaling in the striatum (Lee et al., 2011) and our recent work on the molecular characterization of the protein causing this related disorder showed that it functions in synaptic regulation (Shen et al., in preparation). In addition, PRRT2 was shown in a 2-hybrid screen to interact with a synaptic protein, SNAP25 (Stelzl et al., 2005), raising the possibility that PKD/IC might also result from synaptic dysfunction.

Results

Whole Genome Sequencing

Six samples from six well defined PKD/IC families (K2916, K3323 (Asian), K3538 (African-American), K4874, K4998 and K5471, Caucasian if not otherwise noted) were selected for whole-genome sequencing at Complete Genomics Inc. (CGI). For all the samples, CGI reported overall >50X genome coverage, with >95% of the reference genome called. In the whole genome, the CGI results reported around 500 novel non-synonymous

variants in each Caucasian sample, and 729 and 1202 in the Asian and African-American samples, respectively.

Of note, we have also analyzed the copy number variations (CNVs) and structural variations (SVs) in the PKD/IC region, in order to see if there were genomic level insertions, deletions, duplications, translocations or inversions present in the region (Figure S1). However and as previously reported (Roll et al.), no major CNVs and SVs that were unique and common to the PKD/IC samples were found.

We summarized all the coding variants in the extended critical region from D16S403 to D16S3057 (chr16:22,937,651-57,629,851, NCBI build 37) (Figure S2). Upon initial examination, we did not find a gene with novel non-synonymous variants in all six samples. However, there were several genes with novel non-synonymous variants in two samples, including *TNRC6A*, *PRRT2*, *GDPD3*, *ZNF267* and *NLRC5*. In *PRRT2*, the sample from K5471 showed an insertion of a thymine that would lead to a p.E173X mutation. The sample from K3323 had a C to T transition causing a p.R240X mutation (Figure 1). A closer look at the original read alignments from WGS evidence files in these genes showed that there were two “no-call” (not having enough reads to be significant) cytosine insertions in *PRRT2* (leading to p.R217Pfs*8) in two additional PKD/IC samples from kindreds K2916 and K4998 (Figure 1 and Figure S3). However, Sanger sequencing of *PRRT2* showed that the C insertion was also present in the remaining two PKD/IC samples from kindreds K3538 and K4874 (Figure 1). The reason for the difficulty in calling the C insertion by CGI might be that the insertion was in a stretch of 9 Cs. As CGI uses a 10+25 short read structure (Drmanac et al., 2010), it had a lower chance to cover the whole stretch of 9 or 10 Cs in one read. Thus, all six PKD/IC samples were found to have truncating (frameshift or nonsense) mutations in *PRRT2*.

Further investigation of PRRT2 in probands from 25 clinically well characterized PKD/IC families

Sanger sequencing of the proband from each of the 25 best characterized families in the International PKD/IC Consortium (including the 6 discussed above) revealed mutations in 24 of the 25 probands (Figures 1 and 2). Among these, 21 (K821, K2916, K3446, K3534, K3538, K4874, K4962, K4998, K5118, K5212, K5770, K7716, K7717, K7718, K7719, K7720, K7721, K16719, K18113, K19599, K30085, and WashU) had a 1 base pair (cytosine, C) insertion between bases 649 and 650 (c.649_650insC). This leads to a frame shift and premature protein termination (p.R217Pfs*8, Figure 1 and 2). Two probands (K3323, K7722) harbored a base pair change (C to T) that leads to an immediate stop codon at position 240 (p.R240X, Figures 1 and 2). Another proband (K5471) harbored a 1 base pair (T) insertion between bases 516 and 517 (c.516_517insT), leading to an immediate stop codon (p.E173X, Figure 1). The remaining one pedigree (K8317, not shown) did not harbor any mutation in *PRRT2*.

Testing of probands from 78 less well characterized PKD/IC families

Additional families were available to us for whom we have less clinical data, or for whom additional family members were not available, or for whom the clinical presentation was

somewhat less classic than typical PKD/IC (Bruno et al., 2004). Sanger sequencing of these additional 78 probands for whom the clinical diagnosis was considered less secure revealed an additional 10 (K10615, K50049, K8664, K12206, K50112, K6661, K7920, K9278, K50078, K7253) harboring the p.R217Pfs*8 mutation in familial cases (Figure S4) and 17 with the p.R217Pfs*8 mutation which were isolated cases (data not shown). Finally, one family harbored a novel mutation (1 base pair (T) insertion between bases 980 and 981 (p. 980_981insT), leading to a frame shift and stop codon (p.I327Ifs*14)) (K3391, Figure S4). Taken together, 28 probands of the 78 less well characterized PKD/IC families also had mutations in the *PRRT2* gene.

Examination of normal controls for PRRT novel alleles

We examined the thousand genomes database and the CGI publically available sixty whole genomes for any of the four alleles that we had identified in PKD/IC patients and found them in none of these controls (data not shown). In addition we sequenced an additional two hundred controls and found these alleles in none of them. Thus, these novel alleles were not present in over 2500 control chromosomes.

Conservation of PRRT2 across species

Orthologs of PRRT2 were found in human, gorilla, macaque**,** mouse, guinea pig, dog, cat, dolphin, and zebra fish, but not in *D. melanogaster* and *C. elegans*. By protein sequence alignments, we found that human PRRT2 shared >90% similarity with other primates (gorilla, macaque), ~80% similarity with most mammals, and ~30% similarity with zebra fish (Figure S5). PRRT2 has two predicted transmembrane domains in its C-terminal sequence. Interestingly, the C-terminal sequences of PRRT2 orthologs were extremely conserved across species. Human PRRT2 showed >90% similarity of its C-terminal sequence with other mammals, and ~60% similarity with zebra fish. The high conservation in the region affected by the mutations suggests an important role of this region of the protein in its biological function.

Testing PRRT2 variants for co-segregation with the PKD/IC phenotype

We next tested all available DNAs in the pedigrees harboring *PRRT2* alleles to test for co-segregation. In all but family K3323 where DNAs from multiples affected individuals were available, the mutant alleles co-segregated with the phenotype and with the haplotype whenever previously determined (Figures 1, 2, and S4). In K3323 (Figure 1) there was one “affected” who did not carry the disease allele. In light of the fact that so many of our families co-segregated novel alleles that were not present in a large number of controls, we consider this one individual to be a phenocopy of the PKD/IC phenotype.

Expression of PRRT2 in the central nervous system

HEK293T cells transfected with the N-terminal FLAG fusion protein of hPRRT2 was used as a positive control and untransfected and vector alone transfected HEK293T cells were used as negative controls. Western blots of cell extracts were probed with anti-FLAG antibodies and showed a band of ~65 kDa only in the lane from cells transfected with the clone expressing the FLAG-tagged hPRRT2 fusion protein (Figure S6, lane 11). No band

was present in lanes with extracts from untransfected cells or those transfected with vector alone (lanes 9, 10). In addition, extracts from 8 different mouse tissues were also run on the gel and blotted (lanes 1-8). When the western blot was probed with an antibody against PRRT2, an identical sized band (~65 kDa) was observed in lanes containing extracts from mouse brain and spinal cord (lanes 1 and 8) and the lane with the extract from HEK293 cells containing the FLAG-tagged PRRT2 (lane 11) . No bands were detected in extracts from peripheral mouse tissues tested at this exposure level (Figure S6). At extended exposures, a faint band of the same size was noted in heart extracts (data not shown). Taken together, these data confirm the specificity of the anti-PRRT2 antibody and the localization of PRRT2 in the central nervous system.

PRRT2 interacts with SNAP25

The potential interaction between SNAP25 and PRRT2 defined by a two hybrid screen in a previous report (Stelzl et al., 2005) may be a false positive. Thus we set out to test whether this interaction is valid. The transmembrane protein prediction software (TMHMM Server: http://www.cbs.dtu.dk/services/TMHMM/, TMpred - Prediction of Transmembrane Regions and Orientation protein: http://www.ch.embnet.org/software/TMPRED_form.html) indicated that PRRT2 has 2 putative transmembrane domains at its C-terminus. The site of the p.R217Pfs*8 and other mutations relative to the transmembrane domains are diagrammed (Figure 3A). We preformed *in vitro* co-immunoprecipitation experiments to validate the possible interaction between SNAP25 and PRRT2 in HEK293T cells co-expressing FLAG-tagged SNAP25 and either WT or the mutant form (p.R217Pfs*8) of HA-tagged PRRT2. After pull-down of FLAG-tagged SNAP25 with FLAG antibody, HA-tagged WT PRRT2 can be detected with anti-HA antibody on Western blot of HEK293T extracts co-transfected with FLAG-SNAP25 and WT HA-PRRT2 (Figure 3B). The reciprocal experiment using an anti-HA antibody to pull down tagged Prrt2 demonstrated that SNAP25 could be detected with anti-FLAG antibody (data not shown). Brain extracts from control mice were next used to pull-down Snap25 with anti-Snap25 antibody and after western blotting, Prrt2 could be detected with anti-PRRT2 antibodies (Figure 3C). Taken together, these results indicated that PRRT2 interacts with SNAP25 both *in vitro* and *in vivo*.

Truncated PRRT2 failed to express normally in vitro

Surprisingly, we did not detect obvious expression of mutant HA-PRRT2 (R217Pfs*8) in transfected HEK293T cells (Figure 3B), implying that the mutant form of PRRT2 was either unstable, or did not expressed at all in this heterologous system, and in turn lost its ability to interact with SNAP25. These experiments were next repeated with the 3 other mutant alleles and indicated that all 4 truncation mutations showed remarkably reduced (R240X and I327Ifs*14), or absent (R217Pfs*8 and E173X) expression when transfected alone (Figure 4, left side). When co-transfected with wild-type *PRRT2*, PRRT2 protein was present, suggesting that the mutation did not exert a dominant negative effect on protein levels (Figure 4, right side). This is consistent with the idea that PKD/IC mutations are loss-of-function (haploinsufficiency) and with the single reported case of PKD/IC who harbors a mutation of the *PRRT2* gene (Lipton and Rivkin, 2009).

Cell localization studies

We preformed rat hippocampal neuron cultures transfected with either WT or mutant forms (R217Pfs*8) of PRRT2. PRRT2 was present in thin, MAP2-negative, processes extending from neuron cell bodies that overlap with synapsin positive puncta (Figure 5A and B), as well as synaptophysin and SV2 puncta (data not shown), indicating that it localized predominantly in axons. Importantly, PRRT2 R217Pfs*8, the most common PRRT2 mutation in PKD/IC patients, led to complete abrogration of PRRT2 expression in cultured neurons (Figure 5C). This result matched with our observations in the co-immunoprecipitation experiment above (Figure 3B and Figure 4).

Discussion

PKD/IC is a fascinating disorder combining an infantile form of epilepsy with a paroxysmal and reflex form of movement disorder. The relationship of PD with epileptic seizures has long been suspected and genetic studies demonstrated that PKD and IC share common molecular mechanisms (Szepetowski et al., 1997). Despite intensive and multicenter efforts, the disease gene remained unknown until now. PKD/IC and PNKD appear to be genetically homogeneous; most families with clinically ‘classical’ disease have mutations in the recognized genes (Bruno et al., 2007, and data presented here). *PRRT2* mutations that segregated with the disease were found in nearly all (24/25) of our most well characterized PKD/IC families, including the largest, multigenerational ones. Indeed, previous studies predicted a high level of genetic homogeneity (Bennett et al., 2000; Callenbach et al., 2005; Caraballo et al., 2001; Kikuchi et al., 2007; Lee et al., 1998; Roll et al., ; Swoboda et al., 2000; Szepetowski et al., 1997; Tomita et al., 1999; Weber et al., 2004). The mutations occur in a highly conserved part of the gene, are not present in controls, and lead to near absence of mutant protein expression *in vitro*.

Whether the family with negative screening has a *PRRT2* mutation in noncoding sequences, or deletion of an entire exon has not been excluded. When other smaller and less well characterized PKD/IC families and isolated patients were screened, an important proportion of them were also found to have *PRRT2* mutations. In total, 52/103 of all index cases had mutations in *PRRT2*. Obviously some of the “negative” patients are likely misdiagnosed as having PKD/IC. Others might be different from, albeit similar to, typical PKD/IC. This topic has been discussed in a previous review of a large collection of PKD patients (Bruno et al., 2004); moreover, nongenetic forms of IC and of PKD/IC have been reported (Abe et al., 2000; Camac et al., 1990; Clark et al., 1995; Drake, 1987; Hattori and Yorifuji, 2000; Huang et al., 2005; Mirsattari et al., 1999; Zittel et al., 2011). It is noteworthy that we had previously identified novel *PRRT2* variants in a small number of families but had not pursued them immediately as one did not co-segregate with the disease in K3323. We now know this is the result of a phenocopy in this family.

The present identification of *PRRT2* as the major gene responsible for the syndrome of PKD with IC represents a crucial entry point to elucidate the pathophysiology of this disorder. An interesting aspect of the disease relates to its natural history. The afebrile seizures typically develop in infancy and resolve by the second year of life. The movement disorder can begin from infancy through adolescence and continues through young adult life. However, in a

majority of patients, the movement disorder gets significantly better or completely resolves as patients grow into middle adult life (Bruno et al., 2004). Whether these temporal changes in the expression of the disease are due to developmental differences in the expression of *PRRT2*, epigenetic changes in *PRRT2* with aging, or another cause, remains to be studied. In some PKD/IC patients, seizures can also occur in other contexts (febrile convulsions, generalized seizures in adult patients, etc.). It is not clear if this reflects coincidence of these common disorders with PKD/IC or if PKD/IC lowers the threshold for other forms of epilepsy.

PKD/IC shares striking clinical and genetic similarity with paroxysmal nonkinesigenic dyskinesia (PNKD). PNKD is a related movement disorder in which individuals experience similar dyskinetic attacks that are typically less frequent, longer lasting, and not initiated by sudden movements (Demirkiran and Jankovic, 1995; Tarsy and Simon, 2006). These patients are not recognized to have a related seizure phenotype but may have an increased risk of migraine above the general population (LP, unpublished data) (Bruno et al., 2004; Bruno et al., 2007; Swoboda et al., 2000). In these patients, ingestion of caffeine or alcohol can precipitate attacks which can last for one to four hours (Bruno et al., 2007). Both are highly penetrant, autosomal dominant disorders that exhibit a spectrum of episodic hyperkinetic movements ranging from choreoathetosis (dance-like and writhing movements) to dytonia (movement of limbs, trunk, or face into a fixed position). Between attacks, patients appear completely normal. The dyskinesias typically become evident in childhood, worsen through adolescence, and often improve as patients grow into middle age (Bruno et al., 2004; Bruno et al., 2007). The threshold for inducing attacks in PKD/IC and PNKD is lowered by stress. The clinical similarities between these two disorders suggest the possibility that they may share some similarities at a molecular and pathophysiological level.

Another phenotype similar to PKD/IC and PNKD has been well studied and may occasionally be associated with epilepsy. Paroxysmal exercise induced dyskinesia (PED) is a disorder where individuals experience dyskinesias after prolonged bouts of exercise. All three phenotypes can exhibit clinical dystonia (PNKD as DYT8, PED as DYT9, and PKD/IC as DYT10) (Muller, 2009). The gene for a glucose transporter (GLUT1) has recently been shown to be mutated in some families with PED (Schneider et al., 2009; Suls et al., 2008; Weber et al., 2008). Given the similarities between these 3 disorders, it is interesting to speculate about possible similarities in pathophysiology. Of the 3, most is known about pathophysiology in PNKD with recent insights about the role of the PNKD protein in synaptic regulation and the effect of mutations in dysregulation of dopaminergic signaling (Lee et al., 2004; Shen et al., in preparation). We present circumstantial evidence here suggesting the possibility that PKD/IC may also result from dysfunction of a novel protein in synaptic regulation (through an interaction with SNAP25) though much work remains to either prove or disprove this hypothesis. Finally, what role is a glucose transporter playing in a dyskinesia disorder, particularly one that comes on after prolonged exercise (as opposed to coincident with the onset of movement as in PKD)? One possibility is that an energy dependent process like synaptic regulation of neuronal excitability may initially function normally, but fail if the energy source is insufficient to keep up with the need under conditions of higher neuronal firing rates.

Based on other episodic disorders, it had long been predicted that PKD/IC might be a channelopathy (Ryan and Ptacek, 2010). However, multiple groups have previously ruled out genes from the region known to encode channel related proteins and other physiologically relevant proteins likes those known to function at the synapse. *PRRT2* is a proline-rich protein that was suggested to interact with synaptosomal-associated protein 25 kDa (SNAP25). SNAP25 is a presynaptic membrane protein involved in the synaptic vesicle membrane docking and fusion pathway (Zhao et al., 1994); it plays a pivotal role in calcium triggered neuronal exocytosis (Hu et al., 2002; Sorensen et al., 2002). This is consistent with previous studies on the PNKD protein, which is a novel synaptic protein regulating exocytosis (Shen et al., in preparation) and involved in dopamine signaling (Lee et al., 2011). Interestingly, one atypical patient with deletion of a region encompassing *PRRT2* had not only PKD and possibly infantile-onset convulsions, but also DOPA-responsive parkinsonism (Lipton and Rivkin, 2009). If indeed this deletion causes the phenotype in this patient, it argues for a loss-of-function mechanism. This would be consistent with near absence of protein expression that we saw when expressing the *PRRT2* mutations in HEK293 cells and cultured neurons and with the persistence of protein on Westerns when wild-type and mutant constructs were co-expressed.

Here, we show that PRRT2 localizes to neurons and that the human mutations led to near absence of mutant protein, *in vitro*. This latter observation could be due to nonsense mediated RNA decay. Alternatively, the mRNA and protein may be expressed and translated but degraded very quickly. Such possibilities can be resolved in future work.

Further studies are now needed to understand how and when the disturbance of synaptic functioning leads to a heterogeneous syndrome with episodic, variable and age-dependent cortical and subcortical clinical manifestations. Cloning of the causative gene for this complex disorder has been a Herculean task that has taken nearly 15 years and now the recognition of the causative role of *PRRT2* enables many new lines of experiments that will accelerate the pace of discovery into pathways relevant to the hyperexcitability giving rise to dyskinesias in these patients.

Experimental Procedures

Patient and Family collection

PKD/IC patients and families were collected as previously described (Bennett et al., 2000; Bruno et al., 2004; Caraballo et al., 2001; Lee et al., 2004; Swoboda et al., 2000; Szepetowski et al., 1997; Thiriaux et al., 2002). The country of origin and ancestry of the enrolled research subjects is shown in Table S1.

Whole Genome/Exome Sequencing

Whole-genome sequencing (WGS) was carried out at Completegenomics Inc. (CGI, http://www.completegenomics.com). 15 μg of genomic DNA was submitted for each sample. Front-end data analysis, including sequence mapping and assembly and variant calling, were included in the CGI service. The resulting data from CGI included variant calls (including the original variant calls, their functional annotations and summary by gene), copy number

variation and structural variation calls, and the alignment and coverage files. WGS samples of other diseases studied by our group and the CGI public genomes (http://ftp2.completegenomics.com), 70 genomes in total, were used as controls in this study.

For PKD/IC, we focused on the genomic region between D16S403 and D16S3057 (chr16:22,937,651-57,629,851 based on NCBI build 37), which covered all the critical regions previously reported in PKD/IC linkage analyses. We retrieved all the variants in the genomic region from the WGS results of the PKD/IC samples and reorganized them by their host genes along the chromosome. Variants that were also present in the control genomes were filtered out. We were particularly interested in novel variants that were not present in dbSNP (build 131), control WGS genomes, or the 1000 genome data. Genes with novel non-synonymous variants in multiple samples were given high priority for further examination. We have also examined the additional region from D16S3057 to D16S503, based on a very recent report (Ono et al., 2011) (data not shown).

With the WGS data, we have also examined whether there were copy number variations (CNVs) and structural variations (SVs) common among the PKD/IC samples and not in the control genomes (Figure S7). CGI estimated the copy number based on the normalized counts of reads (read-depth) aligned to genomic regions. The window-width in calculating the CNV is 2 kb. We visualized and compared the CNV results from CGI with the Integrated Genome Viewer (Robinson et al., 2011). We converted the junction data to SVs with cgatools (cgatools.sourceforge.net), and visualized and compared them with custom scripts and Circos (http://circos.ca).

Three members of the Wash U family (Figure 2, Figure S8) were subjected to exome sequencing with Nimblegen SeqCap easy exome capture and either Solexa GAIIx 76-cycle paired-end sequencing or 101-cycle HiSeq. Sequence data was aligned to hg19 with bwa (v0.5.7), optical duplicates marked with Picard (v1.29), and variants extracted using samtools (v0.1.8). Data were filtered for common variants using dbSNP130, 1000 genomes and 8 HapMap individuals as described elsewhere (Harbour et al., 2010).

PCR and Sanger sequencing of DNA samples

PRRT2 was screened for mutations via Sanger sequencing of genomic DNA. Coding regions in DNA of the PKD/IC probands were selected for initial PCR sequencing. Twenty-five microliters of PCR reactions were carried out per 100 ng of genomic DNA and 10 pmol of both forward and reverse primers. Primers were designed outside of splice sites with the intent that intronic sequencing of at least 50 bp would flank each exon border. PCR procedures that lead to successful product amplification were as follows: 98°C, 30 s (98°C, 10 s; 60°C, 30 s; 72°C, 40 s)×35, 72°C, 10 min and 4°C hold. PCR product purification was done using the PCR_{96} Cleanup Plate (Millipore, Bedford, MA, USA) and then sequenced. Exon 2 and exon 4 of PRRT2 are too large to be amplified by a single primer pair, so multiple overlapping primer pairs were used. Exon 2 was broken into three fragments (2A-C), while exon 4 was broken into two (4A-B). All primer sequences and conditions for the four exons are included in Table S2.

Analysis of PRRT2 sequences conservation across species

In order to find homologous genes, the orthologs sequences of PRRT2 across different species were identified from public website database (Ensembl: http://uswest.ensembl.org/index.html, UCSC Genome Bioinformatics: http://genome.ucsc.edu/, and NCBI: http://www.ncbi.nlm.nih.gov/). The ClustalW2 program (http://www.ebi.ac.uk/Tools/msa/clustalw2/) was used for multiple sequence alignment of PRRT2 orthologs. For PRRT2 ortholog C-terminal sequences comparison, the transmembrane protein prediction programs (TMHMM Server: http://www.cbs.dtu.dk/services/TMHMM/, and TMpred - Prediction of Transmembrane Regions and Orientation protein: http://www.ch.embnet.org/software/TMPRED_form.html) were used for prediction of individual PRRT2 C-terminal sequences potentially form the transmembrane domains, then these C-terminal sequences were aligned and compared by the ClustalW2 program.

Cloning of WT and mutant PRRT2

The *PRRT2* plasmid clone (clone ID 5729288) from Open Biosystems (Thermo Scientific, Rockford, IL) was used as the backbone for cloning WT *PRRT2*. The primer sets containing EcoRI and BamHI sites at 5′ and 3′ ends were used to clone WT *PRRT2*. The sequences of cloning primers are listed below: primer-F 5′-ACTGACGAATTCCATGGCAGCCAGCAGCTCT-3′ (with EcoRI site), and primer-R 5′-ACTGACGGATCCTCACTTATACACGCCTAA-3′ (with BamHI site). The WT *hPRRT2* was PCR-amplified from the backbone plasmid, gel-purified with the QIAquick gel extraction kit (Qiagen, Valencia, CA), followed by digestion with EcoRI and BamHI, purified by QIAquick PCR purification kit (Qiagen, Valencia, CA), then cloned into the N-terminal p3XFLAG-CMV-10 expression vector (Sigma-Aldrich, St. Louis, MO) using T4 DNA ligase (Promega, Madison, WI). For cloning *PRRT2* c.649_650insC (PRRT2 R217Pfs*8), site-directed mutagenesis was performed using QuikchangeII site-directed mutagenesis kit (Agilent Technologies, Santa Clara, CA), and the primers for mutagenesis were: mutF1 5′-GGCCCCCCCCCCGAGTGCTGCAG-3′ & mutR1 5′-CTGCAGCACTCGGGGGGGGGGCC-3′ for *PRRT2* c.649_650insC. For transfection of WT and mutant *PRRT* into primary neuronal culture, the N-terminal FLAG-tagged WT and mutant *PRRT* in p3XFLAG-CMV-10 expression vector were used as templates, and re-cloned into the pCAGGS/ES expression vector. The primers for subcloning contained NheI and EcoRV sites at 5′ and 3′ ends, and their sequences are: FLAG-F 5′-ATCGATGCTAGCATGGACTACAAAGACCATGACGGTGATTAT-3′ (with NheI site), and FLAG-R 5′-ATCGATGATATCTCACTTATACACGCCTAAGTTGATGAC-3′ (with EcoRV site).

Western Blotting

Male C57/B6 mice were sacrificed, and different tissues including brain, spinal cord, spleen, kidney, heart, liver, skeletal muscle, and testes were dissected and homogenized in RIPA buffer (10mM Tris-HCl pH 7.2, 150mM NaCl, 5mM EDTA, 1% Triton X-100, 1% SDS, 1% Deoxycholate) with protease inhibitor (Roche, Mannheim, Germany) and phosphatase inhibitor cocktails (Sigma, St. Louis, MO). For positive control of PRRT2 antibody, human embryonic kidney (HEK)-293T cells were transfected with plasmid DNA (p3XFLAG-

PPRRT2 wild type (WT) construct, and p3XFLAG-CMV-10 vector alone) using FuGene HD transfection reagent (Roche Diagnostics GmbH, Mannheim, Germany), grown, and harvested 36 hrs later after transfection. HEK293T cells were then homogenized in 1 mL of RIPA buffer with protease and phosphatase inhibitors. Mouse tissue and HEK293T homogenates were resolved on 10% polyacrylamide gels and electroblotted to nitrocellulose membrane using 50mM Tris-HCl buffer (pH 8.4). The blot was incubated with a rabbit anti-PRRT2 antibody (1:1000, Sigma, St. Louis, MO) overnight at 4°C, then incubated with goat anti-rabbit IgG-HRP (1:5000, Santa Cruz Biotechnology, Santa Cruz, CA) at room temperature for 1 hour, then detected using Immobilon Western Chemiluminescent HRP substrate (Millipore Corporation, Billerica, MA). Blots were stripped and reprobed with a mouse anti-FLAG antibody (1:5000; Sigma, St. Louis, MO), and followed by the procedure describe above.

Co-immunoprecipitation experiment for testing the interaction between SNAP25 and PRRT2

The *SNAP* plasmid clone (clone ID 3867544) from Open Biosystems was used as the backbone for cloning *SNAP25*. The primer sets containing EcoRI and BamHI sites at 5′ and 3′ ends were used to clone *SNAP25*. The sequences of cloning primers are listed below: primer-F 5′-ACTGACGAATTCATGGCCGAAGACGCAGACATGCGCAATG -3′ (with EcoRI site), and primer-R 5′-ACTGACGGATCCTTAACCACTTCCCAGCATCTTTGTTGC-3′ (with BamHI site). *SNAP25* was then cloned into the N-terminal p3XFLAG-CMV-10 expression vector by the procedure described above. The *PRRT2* plasmid clone from Open Biosystems was used as the backbone for cloning N-terminal HA-tagged *PRRT2*. The primer sets containing NcoI and EcoRI sites at 5′ and 3′ ends were used to clone WT HA-tagged *PRRT2*, and the sequences of cloning primers are listed below: primer-F: 5′-CATGCCATGGCATGCATGGCAGCCAGCAGCTCTGAGATCTCTGAG-3′ (with NcoI site), and primer-R: 5′-CCGGAATTCCCGTCACTTATACACGCCTAAGTTGA-3′ (with EcoRI site). *PRRT2* was then cloned into the pEF1-αHA vector (Clontech Laboratories, Inc., Mountain View, CA). The mutant form of N-terminal HA-tagged *PRRT2* (c. 649_650insC, R217Pfs*8) was made from the WT HA-*PRRT2* clone by site-directed mutagenesis described above. HEK293T cells were grown in Dulbecco's modified Eagle's medium (DMEM) supplemented with penicillin, streptomycin, and 10% fetal bovine serum (Invitrogen, Carlsbad, CA) and maintained at 37°C with 5% CO_2. After one day, the cells were split into 10 cm dishes. In parallel, HEK293T cells grown to 80-90% confluence were transfected with DNA (p3XFLAG-CMV-10 SNAP25, pEF1-αHA-*PRRT2*-WT fusion construct, pEF1-αHA-*PRRT2*-c.649_650insC fusion construct, and SNAP25 co-transfected with WT or mutant form of pEF1-αHA-*PRRT2* fusion construct using FuGene HD transfection reagent. Twenty-four to 36 hours after transfection, cells were harvested and homogenized in RIPA buffer containing protease and phosphatase inhibitors. The HEK293T extracts then were applied in the co-immunoprecipitation experiments performed by using an immunoprecipitation kit (Roche, Mannheim, Germany) following the manufacturer's instructions. During the co-immunoprecipitation process, the mouse anti-FLAG M2 monoclonal antibody (1:1000, Sigma, St. Louis, MO) was used to pull-down the FLAG-tagged SNAP25, and rabbit anti-HA tag antibody (1:1000, Abcam, Cambridge, MA) was

subsequently used for detecting HA-PRRT2 fusion proteins in HEK293T cell extracts. The normal mouse IgG (1:1000, Santa Cruz Biotechnology, Santa Cruz, CA) was used as a control of antibody pull-down. For *in vivo* co-immunoprecipitation experiments, whole brains from male C57/B6 mice were homogenized in RIPA buffer with protease inhibitor and phosphatase inhibitor cocktails (3mL/brain). Mouse whole brain extracts were used in co-immunoprecipitation experiments with a kit following the manufacturer's instructions. During the process, rabbit anti-SNAP25 antibody (1:20, Cell Signaling Technology, Danvers, MA) was used to pull-down Prrt2, and rabbit anti-PRRT2 antibody (1:1000) was subsequently used for detecting Prrt2 proteins in mouse whole brain extracts. Rabbit IgG (1:1000, Santa Cruz Biotechnology, Santa Cruz, CA) was used as a control for antibody pull-down. The mouse anti-Syntaxin1 antibody (1:1000, Synaptic Systems GmbH, Goettingen, Germany) was used for detecting Syntaxin1, a known protein partner of Snap25, as a positive control of *in vivo* co-immunoprecipitation.

In vitro degradation experiments of truncated PRRT2

To generate the remaining 3 N-terminal HA-tagged PRRT2 truncation mutation constructs (HA-R240X, HA-E173X, and HA-I327Ifs*14), site-directed mutagenesis was performed using the QuikchangeII site-directed mutagenesis kit described above. HEK293T cells were co-transfected with equal amounts of WT FLAG-PRRT2 construct, and either WT HA-PRRT2 or one of the 4 truncation mutations using FuGene HD transfection reagent. HEK293T cells were grown, and harvested 36 hrs after transfection and then homogenized in 1 mL of RIPA buffer with protease and phosphatase inhibitors. Western blots were performed as described above. A rabbit anti-HA antibody was used for detecting HA-tagged PRRT2, and a mouse anti-FLAG antibody was used to detect FLAG-tagged PRRT2. A mouse anti-GAPDH antibody (1:5000, Millipore, Billerica, MA) was also applied on blots as a loading control.

Primary Neuronal Culture and Immunoflorescence microscopy

Hippocampal neurons were isolated from day 20 rat embryos (E20) in accordance with UCSF IACUC guidelines, transfected with plasmids containing FLAG-tagged WT & mutant human PRRT2 by electroporation (Amaxa), and cultured as previously described (Li et al., 2005). Fixed cells were immunostained with mouse anti-FLAG M2 monoclonal antibody (Sigma, St. Louis, MO) and Rabbit anti-Synapsin (Abcam, Cambridge, MA) or mouse anti-MAP2 (Sigma, St. Louis, MO) antibodies at dilution of 1:500. Alexa488, Alexa 546 (Invitrogen, Carlsbad, CA) and Dylite 549-conjugated secondary antibodies (Jackson ImmunoResearch, West Grove, PA) were used at a dilution of 1:500. Images were obtained using a Zeiss LSM 510 Meta confocal microscope.

Supplementary Material

Refer to Web version on PubMed Central for supplementary material.

Acknowledgments

We thank Dr. Nicholas Lenn for patient referrals. We are grateful to all the families for their participation in this research. This work was supported by grants from the Dystonia Medical Research Foundation, the Bachmann-

Strauss Dystonia Parkinson Foundation, NIH grant U54 RR19481, the Sandler Neurogenetics Fund (Y-HF and LP), NIH grant NS043533 (LP), ANR grant EPILAND (PS), and INSERM. L.J.P. is an investigator of the Howard Hughes Medical Institute.

References

Abe T, Kobayashi M, Araki K, Kodama H, Fujita Y, Shinozaki T, Ushijima H. Infantile convulsions with mild gastroenteritis. Brain & development. 2000; 22:301–306. [PubMed: 10891637]

Bennett LB, Roach ES, Bowcock AM. A locus for paroxysmal kinesigenic dyskinesia maps to human chromosome 16. Neurology. 2000; 54:125–130. [PubMed: 10636137]

Bhatia KP. Paroxysmal dyskinesias. Mov Disord. 2011; 26:1157–1165. [PubMed: 21626559]

Blakeley J, Jankovic J. Secondary paroxysmal dyskinesias. Mov Disord. 2002; 17:726–734. [PubMed: 12210862]

Bruno MK, Hallett M, Gwinn-Hardy K, Sorensen B, Considine E, Tucker S, Lynch DR, Mathews KD, Swoboda KJ, Harris J, et al. Clinical evaluation of idiopathic paroxysmal kinesigenic dyskinesia: new diagnostic criteria. Neurology. 2004; 63:2280–2287. [PubMed: 15623687]

Bruno MK, Lee HY, Auburger GW, Friedman A, Nielsen JE, Lang AE, Bertini E, Van Bogaert P, Averyanov Y, Hallett M, et al. Genotype-phenotype correlation of paroxysmal nonkinesigenic dyskinesia. Neurology. 2007; 68:1782–1789. [PubMed: 17515540]

Callenbach PM, van den Boogerd EH, de Coo RF, ten Houten R, Oosterwijk JC, Hageman G, Frants RR, Brouwer OF, van den Maagdenberg AM. Refinement of the chromosome 16 locus for benign familial infantile convulsions. Clinical genetics. 2005; 67:517–525. [PubMed: 15857419]

Camac A, Greene P, Khandji A. Paroxysmal kinesigenic dystonic choreoathetosis associated with a thalamic infarct. Mov Disord. 1990; 5:235–238. [PubMed: 2388640]

Caraballo R, Pavek S, Lemainque A, Gastaldi M, Echenne B, Motte J, Genton P, Cersosimo R, Humbertclaude V, Fejerman N, et al. Linkage of benign familial infantile convulsions to chromosome 16p12-q12 suggests allelism to the infantile convulsions and choreoathetosis syndrome. American journal of human genetics. 2001; 68:788–794. [PubMed: 11179027]

Clark JD, Pahwa R, Koller C, Morales D. Diabetes mellitus presenting as paroxysmal kinesigenic dystonic choreoathetosis. Mov Disord. 1995; 10:353–355. [PubMed: 7651459]

Demirkiran M, Jankovic J. Paroxysmal dyskinesias: clinical features and classification. Ann. Neurol. 1995; 38:571–579. [PubMed: 7574453]

Drake ME Jr. Paroxysmal kinesigenic choreoathetosis in hyperthyroidism. Postgraduate medical journal. 1987; 63:1089–1090. [PubMed: 3451237]

Drmanac R, Sparks AB, Callow MJ, Halpern AL, Burns NL, Kermani BG, Carnevali P, Nazarenko I, Nilsen GB, Yeung G, et al. Human genome sequencing using unchained base reads on self-assembling DNA nanoarrays. Science (New York, N.Y. 2010; 327:78–81.

Du T, Feng B, Wang X, Mao W, Zhu X, Li L, Sun B, Niu N, Liu Y, Wang Y, et al. Localization and mutation detection for paroxysmal kinesigenic choreoathetosis. J Mol Neurosci. 2008; 34:101–107. [PubMed: 17952630]

Harbour JW, Onken MD, Roberson ED, Duan S, Cao L, Worley LA, Council ML, Matatall KA, Helms C, Bowcock AM. Frequent mutation of BAP1 in metastasizing uveal melanomas. Science (New York, N.Y. 2010; 330:1410–1413.

Hattori H, Yorifuji T. Infantile convulsions and paroxysmal kinesigenic choreoathetosis in a patient with idiopathic hypoparathyroidism. Brain & development. 2000; 22:449–450. [PubMed: 11102731]

Hu K, Carroll J, Fedorovich S, Rickman C, Sukhodub A, Davletov B. Vesicular restriction of synaptobrevin suggests a role for calcium in membrane fusion. Nature. 2002; 415:646–650. [PubMed: 11832947]

Huang YG, Chen YC, Du F, Li R, Xu GL, Jiang W, Huang J. Topiramate therapy for paroxysmal kinesigenic choreoathetosis. Mov Disord. 2005; 20:75–77. [PubMed: 15390133]

Kikuchi T, Nomura M, Tomita H, Harada N, Kanai K, Konishi T, Yasuda A, Matsuura M, Kato N, Yoshiura K, Niikawa N. Paroxysmal kinesigenic choreoathetosis (PKC): confirmation of linkage

to 16p11-q21, but unsuccessful detection of mutations among 157 genes at the PKC-critical region in seven PKC families. Journal of human genetics. 2007; 52:334–341. [PubMed: 17387577]

Lee HY, Nakayama J, Xu Y, Fan X, Karouani M, Shen Y, Pothos EN, Hess EJ, Fu YH, Edwards RH, Ptáček LJ. Dopamine dysregulation in a mouse model of paroxysmal non-kinesigenic dyskinesia. Journal of Clinical Investigation. 2011 In Press.

Lee HY, Xu Y, Huang Y, Ahn AH, Auburger GW, Pandolfo M, Kwiecinski H, Grimes DA, Lang AE, Nielsen JE, et al. The gene for paroxysmal non-kinesigenic dyskinesia encodes an enzyme in a stress response pathway. Hum Mol Genet. 2004; 13:3161–3170. [PubMed: 15496428]

Lee WL, Tay A, Ong HT, Goh LM, Monaco AP, Szepetowski P. Association of infantile convulsions with paroxysmal dyskinesias (ICCA syndrome): confirmation of linkage to human chromosome 16p12-q12 in a Chinese family. Human genetics. 1998; 103:608–612. [PubMed: 9860304]

Li H, Waites CL, Staal RG, Dobryy Y, Park J, Sulzer DL, Edwards RH. Sorting of vesicular monoamine transporter 2 to the regulated secretory pathway confers the somatodendritic exocytosis of monoamines. Neuron. 2005; 48:619–633. [PubMed: 16301178]

Lipton J, Rivkin MJ. 16p11.2-related paroxysmal kinesigenic dyskinesia and dopa-responsive parkinsonism in a child. Neurology. 2009; 73:479–480. [PubMed: 19667324]

Mirsattari SM, Berry ME, Holden JK, Ni W, Nath A, Power C. Paroxysmal dyskinesias in patients with HIV infection. Neurology. 1999; 52:109–114. [PubMed: 9921856]

Muller U. The monogenic primary dystonias. Brain. 2009; 132:2005–2025. [PubMed: 19578124]

Ono S, Yoshiura K, Kurotaki N, Kikuchi T, Niikawa N, Kinoshita A. Mutation and copy number analysis in paroxysmal kinesigenic dyskinesia families. Mov Disord. 2011; 26:761–763. [PubMed: 21312274]

Robinson JT, Thorvaldsdottir H, Winckler W, Guttman M, Lander ES, Getz G, Mesirov JP. Integrative genomics viewer. Nature biotechnology. 2011; 29:24–26.

Rochette J, Roll P, Szepetowski P. Genetics of infantile seizures with paroxysmal dyskinesia: the infantile convulsions and choreoathetosis (ICCA) and ICCA-related syndromes. Journal of medical genetics. 2008; 45:773–779. [PubMed: 19047496]

Roll P, Sanlaville D, Cillario J, Labalme A, Bruneau N, Massacrier A, Delepine M, Dessen P, Lazar V, Robaglia-Schlupp A, et al. Infantile convulsions with paroxysmal dyskinesia (ICCA syndrome) and copy number variation at human chromosome 16p11. PloS one. 5:e13750. [PubMed: 21060786]

Ryan DP, Ptacek LJ. Episodic neurological channelopathies. Neuron. 2010; 68:282–292. [PubMed: 20955935]

Schneider SA, Paisan-Ruiz C, Garcia-Gorostiaga I, Quinn NP, Weber YG, Lerche H, Hardy J, Bhatia KP. GLUT1 gene mutations cause sporadic paroxysmal exercise-induced dyskinesias. Mov Disord. 2009; 24:1684–1688. [PubMed: 19630075]

Sorensen JB, Matti U, Wei SH, Nehring RB, Voets T, Ashery U, Binz T, Neher E, Rettig J. The SNARE protein SNAP-25 is linked to fast calcium triggering of exocytosis. Proceedings of the National Academy of Sciences of the United States of America. 2002; 99:1627–1632. [PubMed: 11830673]

Stelzl U, Worm U, Lalowski M, Haenig C, Brembeck FH, Goehler H, Stroedicke M, Zenkner M, Schoenherr A, Koeppen S, et al. A human protein-protein interaction network: a resource for annotating the proteome. Cell. 2005; 122:957–968. [PubMed: 16169070]

Suls A, Dedeken P, Goffin K, Van Esch H, Dupont P, Cassiman D, Kempfle J, Wuttke TV, Weber Y, Lerche H, et al. Paroxysmal exercise-induced dyskinesia and epilepsy is due to mutations in SLC2A1, encoding the glucose transporter GLUT1. Brain. 2008; 131:1831–1844. [PubMed: 18577546]

Swoboda KJ, Soong B, McKenna C, Brunt ER, Litt M, Bale JF Jr. Ashizawa T, Bennett LB, Bowcock AM, Roach ES, et al. Paroxysmal kinesigenic dyskinesia and infantile convulsions: clinical and linkage studies. Neurology. 2000; 55:224–230. [PubMed: 10908896]

Szepetowski P, Rochette J, Berquin P, Piussan C, Lathrop GM, Monaco AP. Familial infantile convulsions and paroxysmal choreoathetosis: a new neurological syndrome linked to the pericentromeric region of human chromosome 16. American journal of human genetics. 1997; 61:889–898. [PubMed: 9382100]

Tarsy D, Simon DK. Dystonia. N Engl J Med. 2006; 355:818–829. [PubMed: 16928997]

Thiriaux A, de St Martin A, Vercueil L, Battaglia F, Armspach JP, Hirsch E, Marescaux C, Namer IJ. Co-occurrence of infantile epileptic seizures and childhood paroxysmal choreoathetosis in one family: clinical, EEG, and SPECT characterization of episodic events. Mov Disord. 2002; 17:98–104. [PubMed: 11835445]

Tomita H, Nagamitsu S, Wakui K, Fukushima Y, Yamada K, Sadamatsu M, Masui A, Konishi T, Matsuishi T, Aihara M, et al. Paroxysmal kinesigenic choreoathetosis locus maps to chromosome 16p11.2-q12.1. American journal of human genetics. 1999; 65:1688–1697. [PubMed: 10577923]

Weber YG, Berger A, Bebek N, Maier S, Karafyllakes S, Meyer N, Fukuyama Y, Halbach A, Hikel C, Kurlemann G, et al. Benign familial infantile convulsions: linkage to chromosome 16p12-q12 in 14 families. Epilepsia. 2004; 45:601–609. [PubMed: 15144424]

Weber YG, Storch A, Wuttke TV, Brockmann K, Kempfle J, Maljevic S, Margari L, Kamm C, Schneider SA, Huber SM, et al. GLUT1 mutations are a cause of paroxysmal exertion-induced dyskinesias and induce hemolytic anemia by a cation leak. The Journal of clinical investigation. 2008; 118:2157–2168. [PubMed: 18451999]

Zhao N, Hashida H, Takahashi N, Sakaki Y. Cloning and sequence analysis of the human SNAP25 cDNA. Gene. 1994; 145:313–314. [PubMed: 8056350]

Zittel S, Bester M, Gerloff C, Munchau A, Leypoldt F. Symptomatic paroxysmal kinesigenic choreoathetosis as primary manifestation of multiple sclerosis. Journal of neurology. 2011

Highlights

- *PRRT2* is a novel gene, and is mutated in PKD/IC patients
- PRRT2 is expressed in the CNS and interacts with SNAP25
- Truncated forms of PRRT2 are not expressed in cultured cells
- Wild type PRRT2 is in neuronal processes of transfected rat hippocampal neurons

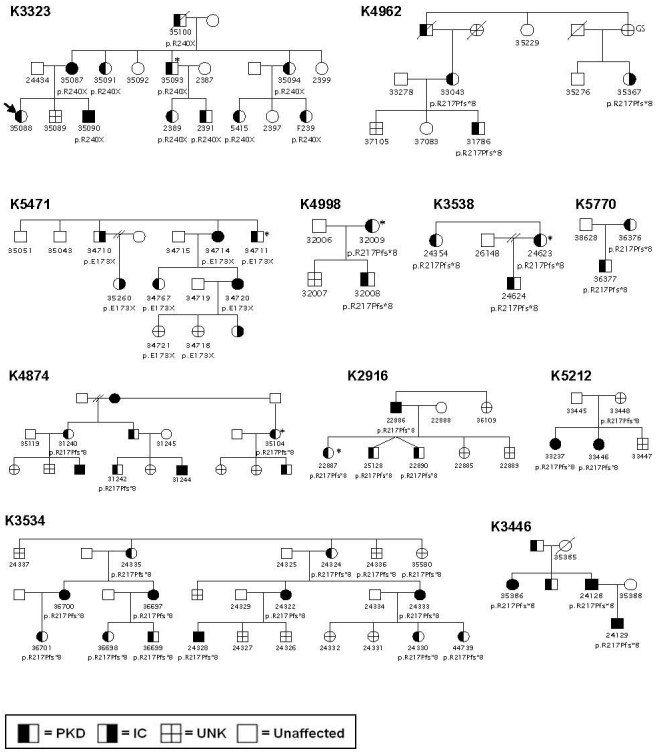

Figure 1. Twenty-four of twenty-five PKD/IC pedigrees with most secure phenotypes carry *PRRT2* mutations

Eleven of these 24 PKD/IC pedigrees are shown. Females are denoted with circles and males with squares. The kindred number is denoted at the upper left corner of each pedigree and the DNA number are noted under individuals where it was available. The specific mutation is denoted under each individual, when present. Individuals with a DNA number but no mutation noted have the wild-type genotype. Affection status for PKD, Infantile Convulsions (under age 2 years), and GS (generalized seizures occurring after age 2 years) are as noted. Samples that were used for WGS are marked with an asterisk (*). One phenocopy was present in K3323 (marked by an arrow).

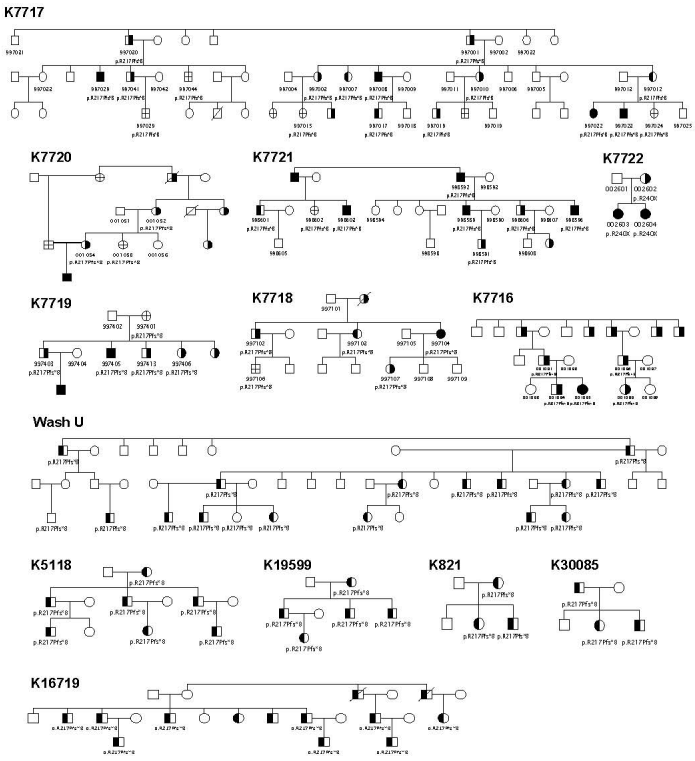

Figure 2. Figure 1: Twenty-four of twenty-five PKD/IC pedigrees with most secure phenotypes carry PRRT2 mutations

Thirteen of these PKD/IC pedigrees are shown. Symbols are as in Figure 1.

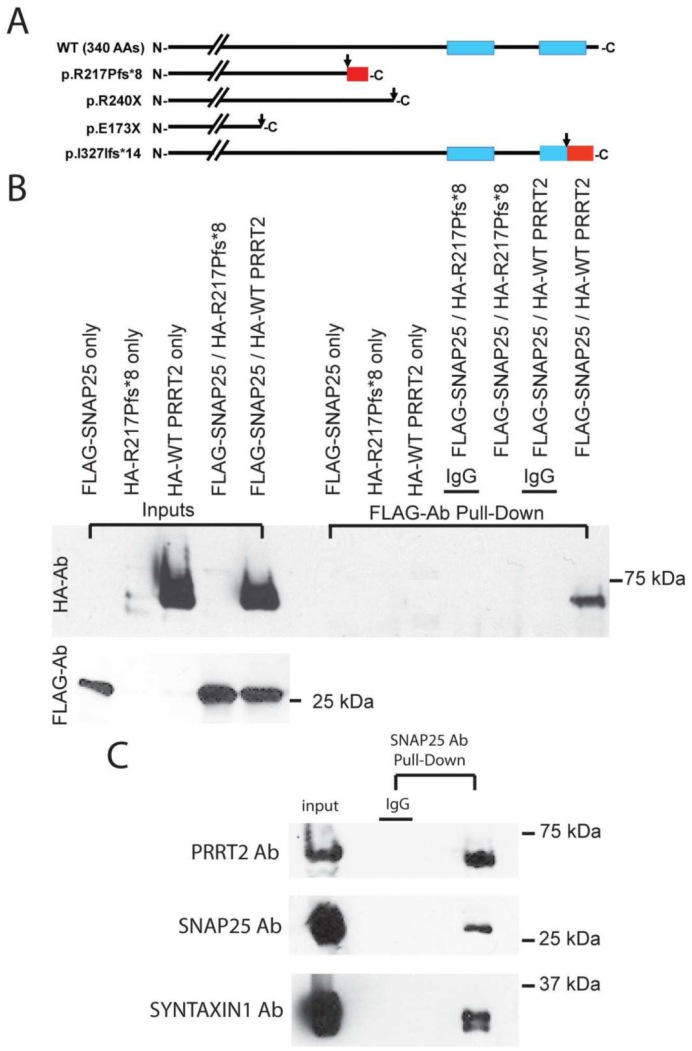

Figure 3. PRRT2 and SNAP25 interact *in vitro* and *in vivo*

(A) The comparison of protein structures for WT and truncated mutants of PRRT2. The blue rectangles represent putative C-terminal transmembrane domains of PRRT2. The black arrows represent positions of mutations producing either nonsense or frameshift mutations. Red rectangles represent novel protein sequences produced by frame shift mutations. **(B)** *In vitro* co-immunoprecipitation was performed in HEK293T cells singly transfected, or co-transfected with FLAG-tagged SNAP25 and either HA-tagged WT or mutant forms (p.R217Pfs*8) of PRRT2. After FLAG antibody pull-down, only the cell extract from HEK293T cells co-transfected with FLAG-tagged SNAP25 and HA-tagged WT PRRT2 showed an ~65 kDa band (upper panel, right-most lane), implying an interaction exists between SNAP25 and PRRT2 *in vitro*. Interestingly, no obvious expression was detected in cell extracts transfected with the mutant form of PRRT2 (upper panel, the second and the fourth lanes from the left). **(C)** *In vivo* co-immunoprecipitation of Snap25 and Prrt2 using whole brain extracts from a control mouse. After SNAP25 antibody pull-down, a Prrt2 band (~65 kDa) was detected using anti-PRRT2 antibody. An antibody specific for SYNTAXIN1, a protein interacting with SNAP25, was also used as a positive control.

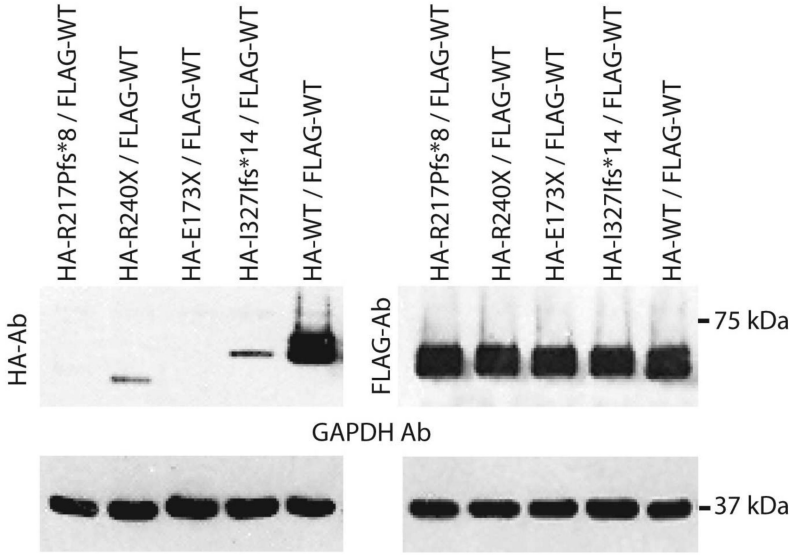

Figure 4. Truncated mutations of *PRRT2* lead to abnormal protein expression *in vitro*

When HEK293T cells were co-transfected with FLAG-tagged PRRT2 and HA-tagged PRRT2, an ~65 kDa band was present when probed with antibody for the tag on the WT fusion protein but FLAG-tagged fusion proteins for the truncation mutations showed a significant reduction (R240X and I327Ifs*14) or undetectable expression (R217pfs*8 and E173X). Thus, the mutations led to low or undetectable PRRT2 protein levels that did not affect the wild type allele *in vitro*. GAPDH antibody was used as a sample loading control.

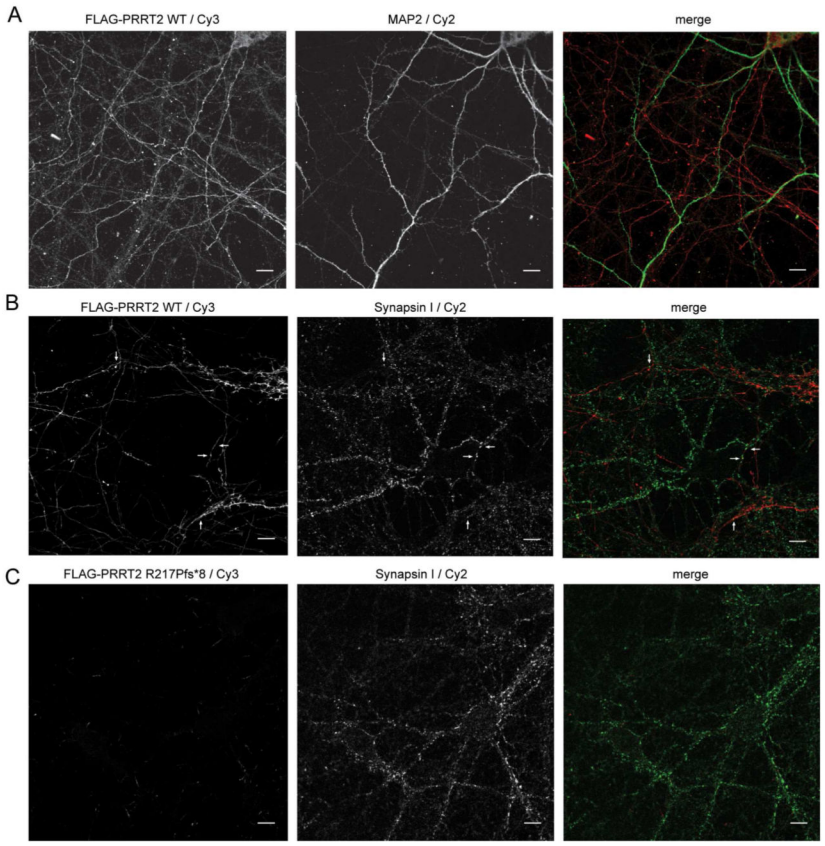

Figure 5. Expression and localization of PRRT2 in hippocampal neurons

(A) Co-immunostaining of WT FLAG-PRRT2 and MAP2 showed distinct localization patterns. **(B)** Co-immunostaining for WT FLAG-PRRT2 and synapsin I showed WT PRRT2 co-localized with synapsin I in neuronal puncta. (C) When co-immunostaining of the FLAG-PRRT2 R217Pfs*8 mutant with synapsin I, no obvious positive staining of mutant PRRT2 was detected. Red= WT FLAG-PRRT2; Green=MAP2 or Synapsin1. Scale bars=10 microns.